

# Bifurcation and dynamics in a mathematical model of early atherosclerosis

## How acute inflammation drives lesion development

Alexander D. Chalmers · Anna Cohen ·  
Christina A. Bursill · Mary R. Myerscough

Received: 3 July 2014 / Revised: 9 February 2015  
© Springer-Verlag Berlin Heidelberg 2015

**Abstract** We present here a mathematical model describing the primary mechanisms that drive the early stages of atherosclerosis. This involves the interactions between modified low density lipoprotein (LDL), monocytes/macrophages, cytokines and foam cells. This model suggests that there is an initial inflammatory phase associated with atherosclerotic lesion development and a longer, quasi-static process of plaque development inside the arterial wall that follows the initial transient. We will show results that show how different LDL concentrations in the blood stream and different immune responses can affect the development of a plaque. Through numerical bifurcation analysis, we show the existence of a fold bifurcation when the flux of LDL from the blood is sufficiently high. By analysing the model presented in this paper, we gain a greater insight into this inflammatory response qualitatively and quantitatively.

**Keywords** Atherosclerosis · Inflammation · PDE model · Bifurcation

**Mathematics Subject Classification** 92C15 · 92C37 · 92C40 · 92C42

### 1 Atherosclerotic plaque formation as the outcome of nonlinear processes

Atherosclerosis (or arteriosclerotic vascular disease) is the primary cause of heart attack (acute myocardial infarction) and stroke (cerebrovascular accident). Together, these are the leading causes of death around the world. It is now accepted that

---

A. D. Chalmers (✉) · A. Cohen · M. R. Myerscough  
The University of Sydney, Camperdown, NSW 2006, Australia  
e-mail: alexander.chalmers@sydney.edu.au

C. A. Bursill  
Heart Research Institute, 7 Eliza Street, Newtown, NSW 2042, Australia

atherosclerosis is a chronic inflammatory response within the intima, the innermost layer of an artery, and that atherosclerosis is driven by the accumulation of macrophage cells within the intima and promoted by modified low density lipoprotein (LDL) particles (Libby 2002; Lusis 2000).

The early stages of atherosclerosis are non-symptomatic. Atherosclerotic lesions, or plaques, can form in the artery wall as early as infancy and continue to grow throughout adulthood. Depending on where the atherosclerotic plaque grows, symptoms may begin to occur, such as numbness or pain in certain parts of the body (examples include angina, peripheral arterial disease and kidney disease). Atherosclerotic lesions stiffen and subsequently weaken the arterial wall and may become unstable and rupture, causing occlusions to blood flow to vital organs which may result in heart attack and stroke.

Plaque formation and growth is the outcome of many nonlinear processes that promote, inhibit or compete with one another. These processes occur on different timescales and in different parts of the tissue. In particular, some processes take place in the lining of the blood vessel and others in the vessel wall. As we are considering this as a continuous process, we represent these processes as a system of partial differential equations (PDEs) and their associated boundary conditions. Many processes can be represented by saturating kinetics, others by bilinear dynamics similar to those of the Law of Mass Action. Logically we expect that atherosclerosis (and certainly models for atherosclerosis) will show characteristic outcomes of nonlinear dynamics, such as loss of steady states through fold bifurcations and hysteresis.

In this paper we focus on early plaque formation and examine both the transient and quasi-steady state behaviour of the model and the bifurcations that it predicts. We interpret these analysis biologically and explore the implications for clinical and medical understanding of plaque growth.

## 2 Early development of an atherosclerotic lesion

### 2.1 Endothelial failure and the formation of modified low density lipoproteins in the intima

A healthy artery is lined by the endothelium, which is a layer of cells that covers the inside of the vessel wall and that significantly contributes to the integrity of the arterial wall. The endothelium can become damaged, particularly in areas of low shear stress, where, for example, there is turbulence or recirculation in the blood flow. This damage may be exacerbated by factors such as hypertension. When the endothelium is injured, LDL, which is present in the blood stream, penetrates the arterial wall and enters the intima. LDL inside the intima is susceptible to modification by free radicals that are produced when the endothelial wall fails (Channon 2002; Furchgott 1999; Napoli et al. 2006).

The failure of the endothelium and the presence of modified LDL trigger the expression of adhesion molecules on the surface of the endothelium. These include selectins (E- and P-selectin) (Hansson and Libby 2006), intercellular adhesion molecules (ICAM-1) and vascular-cell adhesion molecules (VCAM-1) (Libby 2002; Libby

and Ridker 2006). Modified LDL also triggers the production of cytokines such as macrophage colony stimulating factor (M-CSF), monocyte chemoattractant protein 1 (MCP-1) and platelet derived growth factors (PDGF) (Channon 2002; Lusis 2000). Figure 1a illustrates the LDL modification and subsequent stimulation of the endothelium.

## 2.2 Activated species go to work

Endothelial cell adhesion molecules such as VCAM-1 and ICAM-1 enable monocytes from the blood stream in the lumen to attach themselves to the endothelial wall (Lusis 2000). These monocytes migrate into the intima in response to a chemoattractive gradient established by MCP-1 and other cytokines (Han et al. 2004; Hansson and Libby 2006; Newby and Zaltsman 1999).

Monocytes inside the intima differentiate into macrophages in response to macrophage colony stimulating factor (M-CSF) (Libby 2002; Ross 1999). These macrophages begin to exhibit scavenger receptors on their surface which include scavenger receptor A and B1 (SR-A and SR-B1), CD36, CD68, CXCL16 and lectin-type oxidized low-density lipoprotein receptor 1 (LOX1) (Hansson and Libby 2006). Figure 1b illustrates the recruitment and adherence of monocytes to the surface of the endothelium, their subsequent migration into the intima and differentiation into macrophages.

## 2.3 Macrophage ingest modified LDL and promote further inflammation

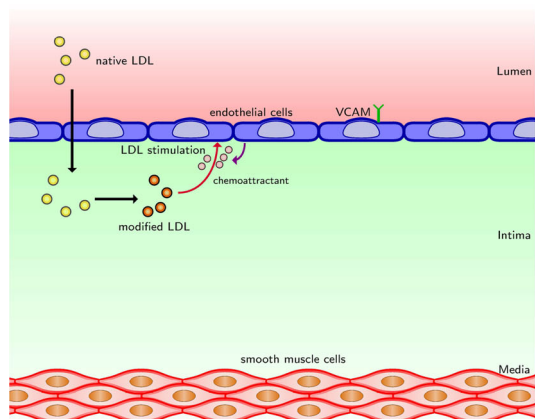
Macrophages that exhibit scavenger receptors recognise modified LDL in the intima and readily internalise the lipid content. Stimulated by their consumption of mod LDL, macrophages secrete chemoattractants, such as MCP-1 and endothelial-stimulating cytokines such as tumour necrosis factor  $\alpha$  (TNF $\alpha$ ) (Hansson and Libby 2006; Libby 2002; Ross 1999). Both chemoattractants and endothelial stimulating (ES) cytokines promote further immigration of monocytes. Macrophages that have consumed lipids, become foam cells, that is, large cells which are filled with lipid droplets that give them a foamy appearance. Foam cells collectively form a fatty streak inside the intima. Figure 1c illustrates the consumption of modified LDL by macrophages, the chemoattractants and ES cytokines produced during this consumption and the resultant cholesterol filled foam cells.

## 3 Previous models: their purpose and structure

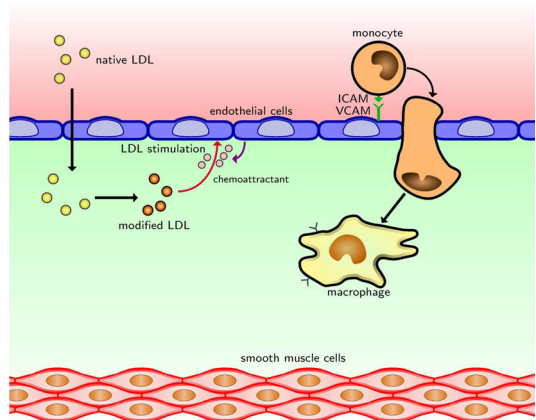
Articles on mathematical and computational models that describe the inflammatory processes in atherosclerosis are starting to proliferate. Each model has its own particular focus, both in how the atherosclerotic plaque and inflammatory processes are represented and in the purpose and results of the modelling.

The simplest approach to atherosclerosis modelling is to ignore plaque spatial structure and take a population-type approach using ordinary differential equation

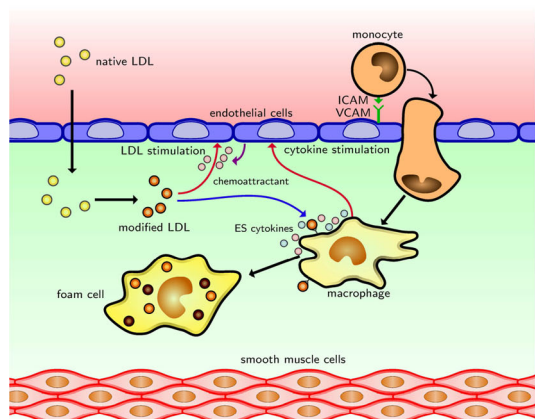
**Fig. 1 a** When the endothelium fails, LDL from the lumen infiltrates the intima. LDL inside the intima is susceptible to modification. The presence of modified LDL at the endothelium triggers the production of monocyte chemoattractants such as MCP-1 and stimulating factors such as M-CSF. This aggravation of the endothelium triggers an expression on the surface of the endothelial wall of adhesion molecules such as VCAM-1 and ICAM-1. **b** Monocytes from the blood stream adhere to the endothelial wall and move into the intima in response to the chemoattractant present in the intima. Once inside the intima, macrophage colony stimulating factor (M-CSF) stimulates the monocytes to differentiate into macrophages and these macrophages display scavenger receptors on their surface. **c** Scavenger expression allows macrophages to consume the modified LDL inside the intima. Macrophages secrete chemoattractants such as MCP-1 and endothelial stimulating cytokines (e.g.,  $\text{TNF}\alpha$ ). As they consume modified LDL, macrophages become foam cells and cease to consume modified LDL.



(a)



(b)



(c)

models. [Ougrinovskaia et al. \(2010\)](#), produced a simple model for inflammation in early atherosclerosis which models modified LDL, macrophages and foam cell populations. The key feature in the model is that macrophage recruitment depends on both modified LDL and the macrophage population in a nonlinear way. Hence, the model has solutions that are bistable, or even multistable, depending on the parameters and the nature of the nonlinearities, so it is possible to have a steady state with low, stable levels of macrophages and a high level of modified LDL and for the same parameter values have an attracting state with no modified LDL (as it has all been consumed) but a mathematically infinite number of macrophages. [Cohen et al. \(2014\)](#) extended this model to include HDL and showed that lipid export is the only mechanism that permits plaque regression, although other actions of HDL reduce the rate of plaque growth.

Simulation models ([Pappalardo et al. 2008](#); [Poston and Poston 2007](#)) also take spatially distributed processes and approximate them by populations averaged across the intima although they may include spatial dimensions along or around the blood vessel. [Pappalardo et al. \(2008\)](#) use a complicated agent-based model which includes immune reactions and macrophage production that occur in the other parts of the body to examine the role of antibodies against oxidised LDL in controlling atherosclerosis. [Poston and Poston \(2007\)](#) use a simple cellular automaton model to explore why atherosclerosis is localised in plaques and not ubiquitous in the vessel lining.

There are many models for blood flow in arteries that seek to determine and explain the location of atherosclerotic plaques (see, for example, [Plank et al. 2007](#)), usually by identifying regions of low shear stress and non-laminar flow in blood vessels. Some models ([Zohdi et al. 2004](#); [Gessaghi et al. 2011](#); [Bulelzai and Dubbeldam 2012](#); [Cilla et al. 2014](#)) seek to link blood flow with modified LDL penetration of the intima. The price of including the effect of blood flow is often a lack of accurate biological detail in the dynamics of events in the intima. In this paper we regard the endothelial injury as a given so that we can carefully examine events on the endothelium and inside the intima. [Bulelzai et al. \(2014\)](#) perform a bifurcation analysis on their ODE models and show that oscillatory solutions are possible but only in a parameter range where the rate of conversion of monocytes into macrophages is two orders of magnitude slower than the rate that macrophages consume modified LDL which modified LDL is plentiful. [Ougrinovskaia et al. \(2010\)](#), in contrast, show that their ODE model has no oscillatory solutions.

Because plaques spread along the length of the blood vessels, models for early atherosclerosis are an obvious application for travelling wave analysis. [El Khatib et al. \(2009, 2007, 2012\)](#) focus on events early in plaque formation and propose a simple two species model where the presence of oxidised LDL draws macrophages across the luminal boundary via a nonlinear boundary condition and the oxidised LDL itself is generated within the intima. They show that there exist travelling waves of inflammation that move along the length of the vessel both when the width of the intima is explicitly modelled and when the width of the intima is assumed to be negligible so that the equations are in only one spatial dimension. [Hidalgo et al. \(2014\)](#) compute solutions of a variant of [El Khatib et al.](#)'s model and show that there is a region of bistability in parameter space where excitatory cytokines and macrophage numbers may either be at a high or at a low steady state.

Calvez et al. (2009) present a similar but more complicated model for early atherosclerotic plaque formation which includes not only macrophages and oxidised LDL but also an activation cytokine that is produced in response to macrophage consumption of oxidised LDL (using a law of mass action model) and stimulates the recruitment of the macrophages at the endothelium. They also include a moving boundary as the intima deforms in response to the accumulation of foam cells. Calvez et al. (2010) use this model, coupled with a model for blood flow to examine how the distortion of the lumen affects blood flow.

Atherosclerosis is an obvious application of free boundary models, although the occlusion of the lumen and the stretching of the outer wall of the blood vessel does not occur to any substantial extent in very early stages of the disease and the determining the details of moving boundary models for plaque growth is not straightforward. Fok (2012) presents a model that represents a chemoattractant which prompts smooth muscle cells to invade from the media. There are several problematic aspects to the model, not least the absence of any lipids in the model and the assumption that the intima thickens in a radially symmetric way rather than only close to the atherosclerotic lesion.

Some models focus on the later stage of atherosclerosis when the plaque has become structured, either by forming a necrotic core or by the invasion of smooth muscle cells that generate a collagen cap. Ibragimov et al. (2005), produce a complicated PDE model for six species that they then simplify to a reduced model for immune cells, cellular debris and chemoattractant. Although the model gives results that appear plausibly similar to the observed pattern of distribution of these quantities in the intima, the reduced model does not include modified LDL and its relation to biological events is not strong. Little et al. (2009) construct a PDE model where there is a necrotic core but no smooth muscle cells or collagen cap, based on a model by McKay et al. (2004), to investigate why low-dose ionising radiation increases the risk of cardiovascular disease. They use the model to examine the effect on inflammation of perturbations from the spatially inhomogeneous steady state that occur when monocytes are killed by radiation. The timescale of the model is, therefore, essentially in hours, rather than the months or years that it takes a plaque to develop from the initial injury.

While the mature plaque is interesting and highly clinically important, models for atherosclerosis will only be built on a sound foundation if we first examine the earliest phase of plaque formation; the processes that are active at the start of plaque formation continue in the mature plaque but other processes and more species are added as plaques get older. It is important, therefore, to generate a biologically sound model for inflammation in the early plaque formation before embarking on more complicated models for the mature plaque.

The model presented here has some similarities with the model presented by Calvez et al. (2009) but takes a more detailed view of the events at the endothelium. We model both the ingress of LDL into the intima and the effect on the endothelium of activation by endothelial injury and the presence of modified LDL inside the vessel wall. We also model the chemotactic flux of macrophages in response to cytokines and modified LDL, both within the intima and across the endothelium and show how events at the endothelium can drive the development of early stage plaques. In particular, we show how transients that follow endothelial injury can settle down to the slow growth of

plaques, a phase that can last for many years. We also show that there can be bistability where the model predicts that the lesion can either be in a highly inflamed state with many macrophages and low levels of modified LDL or less inflamed with a residual level of LDL for the same level of blood LDL and monocyte count. We show that there is a well-defined region of parameter space where this bistability exists.

#### 4 Model development

In this section, we use the description of the mechanisms of early atherosclerosis outlined in Sect. 2, to build a partial differential equation (PDE) model. We will consider five species in this model: modified low density lipoproteins (modified LDL); a chemoattractant (commonly MCP-1 type); an endothelial stimulating (ES) cytokine species (commonly  $\text{TNF}\alpha$  type); the density of monocytes/macrophages; and the density of foam cells.

We do not distinguish, mathematically, between monocytes and macrophages, as we assume that the transition from monocytes to macrophages occurs on a much shorter time scale than other processes. However, in discussing our results, we will call cells “monocytes” when they are in the bloodstream and as they enter the intima and “macrophages” when they are inside the intima. This corresponds to the convention in medical science.

We will also not differentiate between low density lipoprotein types (not modified and modified). We assume that the LDL that enters intima is rapidly modified on a timescale much shorter than the timescale of this model and so we only consider modified LDL. LDL modification been modelled in detail in [Cobbold et al. \(2002\)](#).

We assume that foam cells are immotile in early atherosclerosis and as such have no spatial terms and as such, have no flux boundary conditions.

The model comprises equations for the following quantities:

- $\tilde{\ell}(\mathbf{x}, t)$  the concentration of modified LDL;
- $p(\mathbf{x}, t)$  the concentration of chemoattractants;
- $q(\mathbf{x}, t)$  the concentration of ES cytokines;
- $m(\mathbf{x}, t)$  the density of monocytes/macrophages; and
- $N(\mathbf{x}, t)$  the density of foam cells.

We use a tilde to indicate variables and parameters that will be rescaled in Sect. 4.2.

Each of these dependent variables is a function of position,  $\mathbf{x}$ , and time,  $t$ . We assume that the inflammatory process occurs inside a bounded domain  $\Omega$ , which may be a subset of  $\mathbb{R}$ ,  $\mathbb{R}^2$  or  $\mathbb{R}^3$ . We define  $\Gamma_1$  as the part of the boundary of  $\Omega$  which corresponds to the interface between the lumen and the intima. We define  $\Gamma_2$  as the part of the boundary on  $\Omega$  that corresponds to the interface between the intima and the media, which is the next layer outwards in the arterial wall. Moreover, we assume that none of the species are present before the endothelium is compromised and that the medial boundary does not contribute to the initial inflammatory processes.

Thus we have the following initial conditions

$$\tilde{\ell}(\mathbf{x}, 0) = 0 \quad p(\mathbf{x}, 0) = 0 \quad q(\mathbf{x}, 0) = 0 \quad m(\mathbf{x}, 0) = 0 \quad N(\mathbf{x}, 0) = 0. \quad (1)$$

The boundary conditions on the medial boundary  $\Gamma_2$  are

$$(\hat{\mathbf{n}} \cdot \mathbf{J}_{\tilde{\ell}})_{\Gamma_2} = 0 \quad (\hat{\mathbf{n}} \cdot \mathbf{J}_p)_{\Gamma_2} = 0 \quad (\hat{\mathbf{n}} \cdot \mathbf{J}_q)_{\Gamma_2} = 0 \quad (\hat{\mathbf{n}} \cdot \mathbf{J}_m)_{\Gamma_2} = 0.$$

where  $\hat{\mathbf{n}}$  is the relevant outward unit normal to the surface.

This assumes that no cells, modified LDL or cytokines pass from the intima into the media or vice versa.

The boundary conditions on the luminal boundary  $\Gamma_1$  are complicated and key to the dynamics of the model. We specify boundary conditions on  $\Gamma_1$  in Sect. 4.1 along with the differential equations for interactions within the intima.

## 4.1 Model equations

### 4.1.1 Modified LDL ( $\tilde{\ell}$ )

Within the intima, the concentration of modified LDL is modelled by

$$\frac{\partial \tilde{\ell}}{\partial t} = \underbrace{\tilde{D}_{\tilde{\ell}} \nabla^2 \tilde{\ell}}_{\text{Diffusion}} - \underbrace{\tilde{\mu}_{\tilde{\ell}} \frac{m \tilde{\ell}}{\alpha + \tilde{\ell}}}_{\text{Consumption}} - \underbrace{\tilde{d}_{\tilde{\ell}} \tilde{\ell}}_{\text{Decay}}. \quad (2)$$

The first term on the right hand side of this equation describes diffusion of modified LDL (Dabagh et al. 2009). The next term describes the loss of modified LDL within the intima due to consumption by macrophages. We model this as linear in macrophage density,  $m$ , but saturating in modified LDL concentration,  $\tilde{\ell}$ , as it is likely that there is an upper limit to the rate that modified LDL can be consumed by each macrophage. We use a Michaelis–Menten-type function as it is the simplest way to represent saturating dynamics. It is reasonable to expect that macrophages will consume modified LDL at a rate proportional to  $\tilde{\ell}$  at low concentrations of modified LDL and the function  $\tilde{\ell}/(\alpha + \tilde{\ell})$  is linear close to  $\tilde{\ell} = 0$ . The last term is a linear decay term, which represents other losses of modified LDL, perhaps through degradation. We choose  $\tilde{d}_{\tilde{\ell}}$  so that this term is an order of magnitude smaller than the other terms in Eq. (2).

We divide the luminal boundary  $\Gamma_1$  into two subsets,  $\Gamma_3$  and  $\Gamma_4$ . On  $\Gamma_3$  we assume that the endothelium has been compromised so that there is a flux of LDL into the domain (the intima) We assume this LDL is immediately modified and that LDL influx and modification can be represented as a single process by a flux of modified LDL. This flux of modified LDL on  $\Gamma_3$  is given by

$$(\hat{\mathbf{n}} \cdot \mathbf{J}_{\tilde{\ell}})_{\Gamma_3} = -\tilde{\sigma}_{\tilde{\ell}}. \quad (3)$$

This boundary condition assumes that the flux of modified LDL across the endothelial wall is constant and that the only controlling factor is the physical failure of the endothelial wall. We take  $\Gamma_4 = \Gamma_1 \setminus \Gamma_3$  as the section of endothelium that is not injured. We assume that no LDL permeates the healthy endothelial wall, so the boundary condition on  $\Gamma_4$  is

$$(\hat{\mathbf{n}} \cdot \mathbf{J}_{\tilde{\ell}})_{\Gamma_4} = 0. \tag{4}$$

In the analysis of this model, we will only use one spatial dimension across the width of the intima. The endothelial boundary must either be undamaged or damaged, however, it can only be divided into damaged and undamaged subsets in two or three spatial dimensions. Hence, in our analysis, we assume the endothelial boundary is damaged (see Sect. 4.2).

#### 4.1.2 Monocyte chemoattractants ( $p$ )

Within the intima, the concentration of monocyte chemoattractants is modelled by

$$\frac{\partial p}{\partial t} = \underbrace{\widetilde{D}_p \nabla^2 p}_{\text{Diffusion}} + \underbrace{\widetilde{\mu}_p \frac{m\tilde{\ell}}{\alpha + \tilde{\ell}}}_{\text{Production}} - \underbrace{\widetilde{d}_p p}_{\text{Decay}}. \tag{5}$$

The first term on the right hand side of this equation, represents the diffusion of chemoattractants. This is large compared to diffusion of modified LDL and random motion of monocytes/macrophages (Sect. 4.1.4) because cytokine molecules are much smaller and lighter than both LDL particles and macrophages. The next term defines the production of chemoattractants by macrophages at a rate proportional to their consumption of modified LDL. The last term is a linear decay term, which models other losses and, as with modified LDL, is at least an order of magnitude smaller than the other terms in Eq. (5).

At the endothelial boundary  $\Gamma_1$ , the flux of chemoattractants ( $p$ ) is modelled by

$$(\hat{\mathbf{n}} \cdot \mathbf{J}_p)_{\Gamma_1} = - \left( \widetilde{\sigma}_{p1} \frac{\tilde{\ell}}{\beta_p + \tilde{\ell}} + \widetilde{\sigma}_{p2} q \right). \tag{6}$$

Chemoattractants such as MCP-1 are produced at the endothelium in response to stimulation by modified LDL (Lusis 2000). This is described by the first term on the right hand side of (6). We assume that the rate of chemoattractant production saturates as modified LDL concentration increases. We also assume that ES cytokines enhance the production of chemoattractant by endothelial cells. This is described by the second term in (6) so the flux of chemoattractants from the endothelium into the intima increases as the concentration of ES cytokines increases at the endothelium (Hansson and Libby 2006; Volpert and Petrovskii 2009).

#### 4.1.3 ES cytokines ( $q$ )

Within the intima, the rate of change of ES cytokine concentration is modelled by

$$\frac{\partial q}{\partial t} = \underbrace{\widetilde{D}_q \nabla^2 q}_{\text{Diffusion}} + \underbrace{\widetilde{\mu}_q \frac{m\tilde{\ell}}{\alpha + \tilde{\ell}}}_{\text{Production}} - \underbrace{\widetilde{d}_q q}_{\text{Decay}}. \tag{7}$$

The first term on the right hand side models diffusion of ES cytokines. The diffusion rate of ES cytokines is similar to the diffusion rate of chemoattractant concentration  $p$ . The next term represents the production of ES cytokines under the same assumptions as the production of chemoattractants. The last term is a linear decay term that models generic ES cytokine loss in the intima.

At the endothelial boundary  $\Gamma_1$ , the flux of ES chemokines ( $q$ ) is modelled by

$$(\hat{\mathbf{n}} \cdot \mathbf{J}_q)_{\Gamma_1} = \tilde{\sigma}_q q. \tag{8}$$

ES chemokines occur at detectable levels in the bloodstream (McKellar et al. 2009; Pai et al. 2004). The cytokines may or may not have atherosclerotic origins, but it is reasonable to impose a small outward flux of ES cytokines from the intima to the lumen.

#### 4.1.4 Monocytes/macrophages ( $m$ )

Within the intima, the density of macrophages is modelled by

$$\frac{\partial m}{\partial t} = \underbrace{\widetilde{D}_m \nabla^2 m}_{\text{Random movement}} - \underbrace{\nabla \cdot (\widetilde{\chi}_m m \nabla \ell)}_{\text{Chemotaxis}} - \underbrace{\widetilde{\mu}_m \frac{m \ell}{\alpha + \ell}}_{\text{Conversion to foam cells}} - \underbrace{\widetilde{d}_m m}_{\text{Decay}}. \tag{9}$$

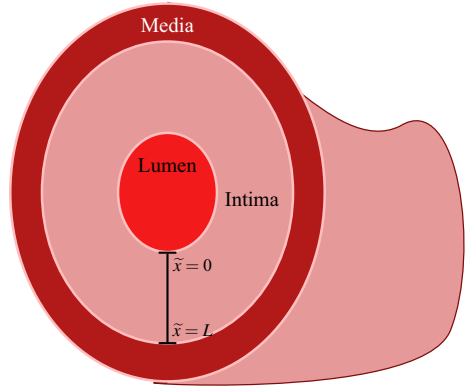
The first term on the right hand side of this equation models the random movement of macrophages within the intima. As macrophages are relatively large, we assume that this is slow compared to diffusive movement of LDL and cytokines in the intima. The next term describes chemotactic motion of macrophages in response to modified LDL. We assume that the chemotactic coefficient,  $\widetilde{\chi}_m$ , is constant throughout the intima. The third term describes the rate of conversion of macrophages to foam cells in the intima after the consumption of modified LDL. This is similar to the modified LDL consumption term discussion in Sect. 4.1.1. The last term is a small linear decay term that accounts for other losses and cell death and, perhaps, dedifferentiation.

The boundary conditions for monocytes/macrophages ( $m$ ) is

$$(\hat{\mathbf{n}} \cdot \mathbf{J}_m)_{\Gamma_3} = -\widetilde{\sigma}_m (1 + A_0 q)(p - P_0)H(p - P_0) \tag{10}$$

where  $H(p - P_0)$  is the Heaviside function. This models macrophage migration into the intima in response to a chemoattractant gradient across the endothelium. We assume that monocytes can only enter the intima at the site of injury,  $\Gamma_3$  (as defined in Sect. 4.1.1), the only site of the endothelium at which monocytes adhere to. Mathematically, we model this gradient as the difference between the concentration of chemoattractant in the bloodstream  $P_0$  and the concentration of chemoattractant at the endothelium. This boundary condition is similar to the condition for heat loss through a poorly conducting boundary. Monocyte presence and adhesion to the endothelium is enhanced by the ES cytokines that are present at the boundary. We assume that the more monocytes that adhere to the endothelium, the more that will migrate into

**Fig. 2** The cross section of an artery showing the domain of the model. The size of the intima is exaggerated



the intima. We assume that the migration of monocytes through the endothelial wall depends on the concentration of ES chemokines,  $q$ , and we choose a linear expression to model this. We assume that monocytes can not adhere to healthy endothelial cells, so the boundary condition on  $\Gamma_4 = \Gamma_1 \setminus \Gamma_3$  is

$$(\hat{\mathbf{n}} \cdot \mathbf{J}_m)_{\Gamma_4} = 0 \tag{11}$$

#### 4.1.5 Foam cells ( $N$ )

We assume that within the intima, the rate that macrophages undergo conversion through lipoprotein consumption to become foam cells is proportional to macrophage consumption of modified LDL and hence:

$$\frac{\partial N}{\partial t} = \widetilde{\mu}_m \frac{m\tilde{\ell}}{\alpha + \tilde{\ell}}. \tag{12}$$

We assume that foam cells are immotile and so don't have flux boundary conditions.

#### 4.2 Rescaled equations on a one dimensional domain

We take the domain as the one dimensional segment through the intima, bounded by the lumen (at  $\tilde{x} = 0$ ) and the media (at  $\tilde{x} = L$ ) (see Fig. 2). We rescale time ( $t$ ), space ( $\tilde{x}$ ) and modified LDL concentration  $\tilde{\ell}$  as follows

$$\tau = rt \quad x = \frac{\tilde{x}}{L} \quad \ell = \frac{\tilde{\ell}}{\alpha},$$

where  $r$  is dependent on the timescale considered (see Sect. 4.3) and  $L$  is the width of the intima. The parameter  $\alpha$  controls the saturation rate of modified LDL consumption as  $\tilde{\ell}$  increases. We assume that the effects of curvature on the flux boundary conditions at the endothelium are negligible because the width of the intima ( $L$ ) is much less than the radius of the lumen.

The rescaled equations in one spatial dimensional are

$$\frac{\partial \ell}{\partial \tau} = D_\ell \frac{\partial^2 \ell}{\partial x^2} - \mu_\ell \frac{m\ell}{1 + \ell} - d_\ell \ell, \tag{13}$$

$$\frac{\partial p}{\partial \tau} = D_p \frac{\partial^2 p}{\partial x^2} + \mu_p \frac{m\ell}{1 + \ell} - d_p p, \tag{14}$$

$$\frac{\partial q}{\partial \tau} = D_q \frac{\partial^2 q}{\partial x^2} + \mu_q \frac{m\ell}{1 + \ell} - d_q q, \tag{15}$$

$$\frac{\partial m}{\partial \tau} = D_m \frac{\partial^2 m}{\partial x^2} - \chi_m \frac{\partial}{\partial x} \left( m \frac{\partial \ell}{\partial x} \right) - \mu_m \frac{m\ell}{1 + \ell} - d_m m, \tag{16}$$

$$\frac{\partial N}{\partial \tau} = \mu_m \frac{m\ell}{1 + \ell}, \tag{17}$$

with boundary conditions at  $x = 0$ :

$$D_\ell \frac{\partial \ell}{\partial x}(0, \tau) = -\sigma_\ell, \tag{18}$$

$$D_p \frac{\partial p}{\partial x}(0, \tau) = -\sigma_{p1} \frac{\ell}{\beta_p + \ell} - \sigma_{p2} q, \tag{19}$$

$$D_q \frac{\partial q}{\partial x}(0, \tau) = \sigma_q q, \tag{20}$$

$$D_m \frac{\partial m}{\partial x}(0, \tau) - \chi_m m \frac{\partial \ell}{\partial x}(0, \tau) = -\sigma_m (1 + A_0 q)(p - P_0) H(p - P_0), \tag{21}$$

and boundary conditions at  $x = 1$

$$\begin{aligned} D_\ell \frac{\partial \ell}{\partial x}(1, \tau) = 0, \quad D_p \frac{\partial p}{\partial x}(1, \tau) = 0, \quad D_q \frac{\partial q}{\partial x}(1, \tau) = 0, \\ D_m \frac{\partial m}{\partial x}(1, \tau) - \chi_m m \frac{\partial \ell}{\partial x}(1, \tau) = 0. \end{aligned} \tag{22}$$

The initial conditions are

$$\ell(x, 0) = 0, \quad p(x, 0) = 0, \quad q(x, 0) = 0, \quad m(x, 0) = 0, \quad N(x, 0) = 0. \tag{23}$$

The rescaled parameters are

$$\begin{aligned} D_\ell &= \frac{\widetilde{D}_\ell}{rL^2}, & \mu_\ell &= \frac{\widetilde{\mu}_\ell}{r\alpha}, & d_\ell &= \frac{\widetilde{d}_\ell}{r}, & \sigma_\ell &= \frac{\widetilde{\sigma}_\ell}{rL\alpha}, \\ D_p &= \frac{\widetilde{D}_p}{rL^2}, & \mu_p &= \frac{\widetilde{\mu}_p}{r}, & d_p &= \frac{\widetilde{d}_p}{r}, & \sigma_{p1} &= \frac{\widetilde{\sigma}_{p1}}{rL}, \\ \sigma_{p2} &= \frac{\widetilde{\sigma}_{p2}}{rL}, & \beta_p &= \frac{\widetilde{\beta}_p}{\alpha}, & & & & \\ D_q &= \frac{\widetilde{D}_q}{rL^2}, & \mu_q &= \frac{\widetilde{\mu}_q}{r}, & d_q &= \frac{\widetilde{d}_q}{r}, & \sigma_q &= \frac{\widetilde{\sigma}_q}{rL}, \end{aligned}$$

**Table 1** Values for parameters whose values can be estimated from evidence external to the model

Parameter	Value	Source
$\widetilde{D}_p$	$\sim 100 \mu\text{m}^2/\text{s}$	Paavola et al. (1998)
$\widetilde{D}_q$	$\sim 100 \mu\text{m}^2/\text{s}$	Assumed same as $\widetilde{D}_p$
$\widetilde{D}_\ell$	$2.13 \mu\text{m}^2/\text{s}$	Dabagh et al. (2009)
$L$	$\sim 40 \mu\text{m}$	Di Vito et al. (2013)

**Table 2** Rescaled parameters from Table 1 and values of unknown parameters that can be estimated using order of magnitude assumptions in the model

Parameter	Value	Reason
$D_\ell$	$10^3$	From Table 1
$D_p$	$10^5$	From Table 1
$D_q$	$10^5$	From Table 1
$D_m$	$10^{-1}$	$D_m \ll D_\ell$

$$D_m = \frac{\widetilde{D}_m}{rL^2}, \quad \chi_m = \frac{\widetilde{\chi}_m \alpha}{rL^2}, \quad \mu_m = \frac{\widetilde{\mu}_m}{r}, \quad d_m = \frac{\widetilde{d}_m}{r},$$

$$\sigma_m = \frac{\widetilde{\sigma}_m}{rL}$$

### 4.3 Parameters of interest and parameter values

There are 24 constants in the model, most of which are unknown. In some cases, this is due to the difficulty of measuring these parameters either in vivo or even in vitro. In other cases, there has been no apparent need to measure these parameters. Since experimental work in atherosclerosis is usually carried out in vivo using animal models, measuring reaction rates and fluxes is difficult, expensive and time consuming and so there usually has to be a demonstrated need for a measurement before it is made. However, some values for  $D_p$ ,  $D_q$ ,  $D_\ell$  and  $L$  are known from experimental data (Table 1).

We take  $r = 6 \times 10^{-7}$  which converts the timescale of the model into the order of weeks (one time unit represents approximately 19 days), rather than seconds. As we know little about the other constants in this model, we will represent all of the constants by some relative order of magnitude (Table 2).

We will explore the effect of two parameters in particular:  $\sigma_\ell$  which controls the rate that modified LDL enters the intima from the lumen; and  $\sigma_m$  which controls the rate of migration of monocytes into the intima. These parameters model effects that are believed to trigger inflammation at the endothelium and drive lesion formation in the intima. We present numerical results for different values of  $\sigma_\ell$  and  $\sigma_m$ .

The parameter  $\sigma_\ell$  is important as we assume that the magnitude of  $\sigma_\ell$  is related to the concentration of LDL in the blood and the severity of the injured endothelium. The parameter  $\sigma_m$  corresponds to the number of monocytes in the blood stream and their ability to adhere to the endothelium, both related to the underlying levels of

**Table 3** Estimates for unknown parameters for use in the model.

We take  $\mu_\ell$ ,  $\mu_p$  and  $\mu_q$  to be much larger than  $\mu_m$  as we assume that macrophages need a large quantity of modified LDL to convert into foam cells and that a large amount of chemoattractants and cytokines are secreted per macrophage

Parameter	Value
$\mu_\ell$	$10^5$
$d_\ell$	$10^1$
$\mu_p$	$10^5$
$d_p$	$10^1$
$\mu_q$	$10^5$
$d_q$	$10^1$
$\chi_m$	$10^{-1}$
$\mu_m$	$10^2$
$d_m$	$10^{-1}$
$\sigma_{p1}$	$10^4$
$\sigma_{p2}$	$10^3$
$\beta_p$	$10^0$
$\sigma_q$	$10^0$
$P_0$	$10^{-1}$
$A_0$	$10^{-2}$

inflammation in the body. This may be high due to inflammation elsewhere in the body, for example, Type 1 diabetes, arthritis or any other trauma within the body.

The values for the other parameters in the model are given in Table 3.

## 5 Time Dependent Solutions of the Model

In Figures 3 and 4 we present results for the concentration of modified LDL at the endothelium,  $\ell(0, \tau)$  and the concentration of chemoattractant at the endothelium,  $p(0, \tau)$ , each as a function of the rescaled time variable,  $\tau$ . The variables,  $p$  and  $\ell$  take their maximum on the endothelial boundary, i.e.,  $x = 0$  (Fig. 5), so the value at the endothelium provides a good measure of the solution. Additionally, in Figs. 3 and 4, we show the monocyte migration rate into the intima, which is given by  $\sigma_m(1 + A_0q(0, \tau))(p(0, \tau) - P_0)H(p(0, \tau) - P_0)$ . These three measures are important drivers of atherogenesis. To complete Figs. 3 and 4, we include results for the total number of macrophages, the total consumption rate of modified LDL and the total number of foam cells in the intima. Mathematically, these are integrals of  $m$ ,  $\frac{\ell m}{1 + \ell}$  and  $N$  respectively over the rescaled spatial domain of the intima.

In general, the results show that there are transient changes in all the variables immediately following the injury. This transient behaviour settles to a quasi-steady state after some time, which depends on the parameters used. At quasi-steady state, the modified LDL concentration,  $\ell$ , the density of macrophages,  $m$ , the concentration of chemoattractants,  $p$  and the concentration of ES cytokines,  $q$ , do not change with

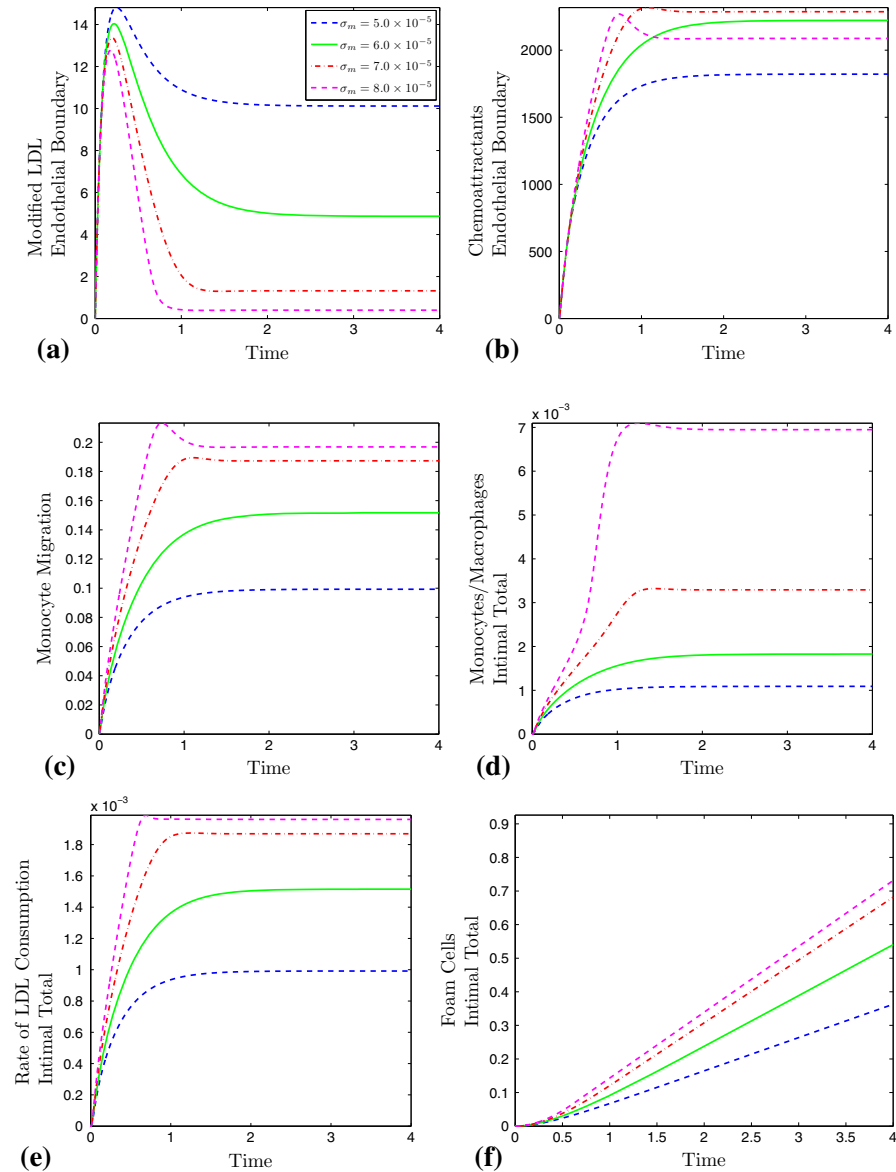


**Fig. 3** Examples of the development of lesions as a function of time, immediately after injury when the inward flux of modified LDL is low ( $\sigma_\ell = 2 \times 10^2$ ) for various values of  $\sigma_m$  between 5 and  $8 \times 10^{-5}$ . (Blue dashed line  $\sigma_m = 5 \times 10^{-5}$ , green solid line  $\sigma_m = 6 \times 10^{-5}$ , red dot-dash line  $\sigma_m = 7 \times 10^{-5}$ , magenta dashed line  $\sigma_m = 8 \times 10^{-5}$ .) **a** Concentration of modified LDL on the endothelial boundary; **b** chemoattractant concentration at the endothelial boundary; **c** monocyte migration rate through the endothelium; **d** total density of monocytes/macrophages in the intima; **e** rate of consumption of modified LDL by macrophages across the intima; **f** total density of foam cells in the intima

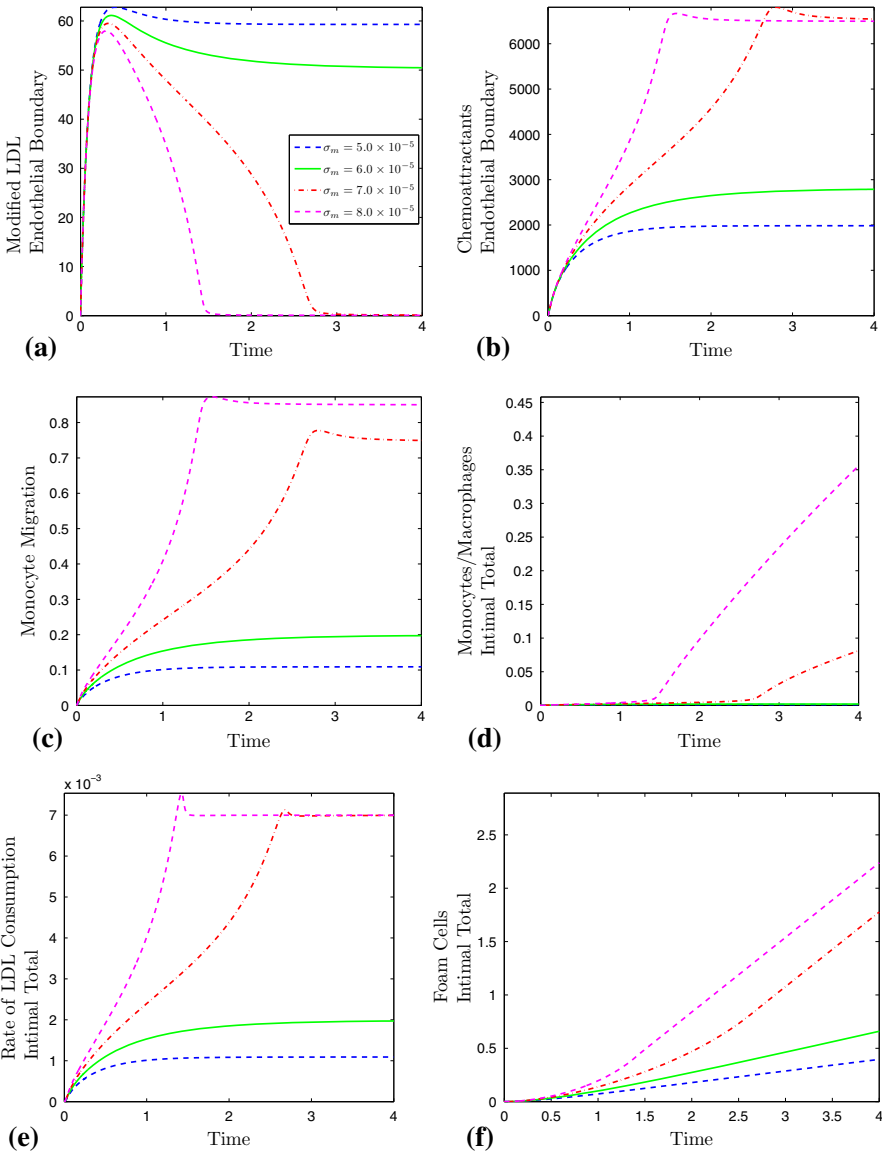


**Fig. 4** This figure shows analogous plots to Fig. 3 of time courses immediately following injury for the same values of  $\sigma_m$  but when the modified LDL flux is high ( $\sigma_\ell = 7 \times 10^2$ ). See Fig. 3 caption for explanation of subplots

time. However, the foam cell density,  $N$ , continues to increase with time. Therefore we refer to the consumption rate of modified LDL as a measure of foam cell production that achieves a non-zero steady state.

Figure 3 shows results for varying values of  $\sigma_m$  in the range  $5 \times 10^{-5}$  to  $8 \times 10^{-5}$  when  $\sigma_\ell = 2 \times 10^2$ , a low value for the model.

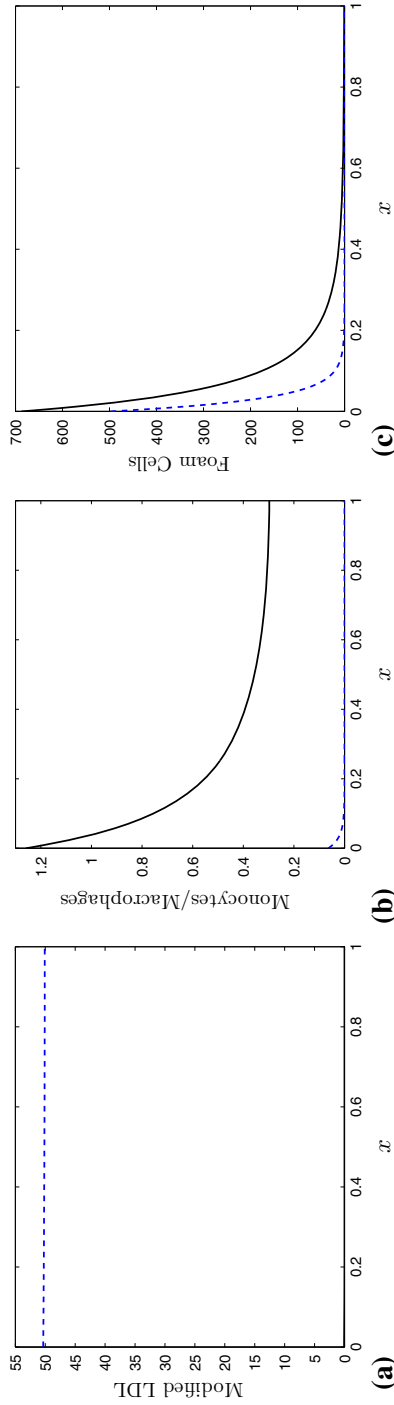


**Fig. 5** Spatial pattern at quasi-steady state for  $\sigma_\ell = 7 \times 10^2$  and  $\sigma_m$  values  $6.0 \times 10^{-5}$  (blue dashed curve) and  $7.0 \times 10^{-5}$  (black solid curve). These show that the maximum values of  $\ell$ ,  $m$  and  $N$  occur at the endothelial boundary,  $x = 0$ . **a** Modified LDL concentration; **b** macrophage density; **c** foam cell density

Initially, the concentration of modified LDL at the endothelial boundary increases for every value of  $\sigma_m$ . However, once a significant number of monocytes have migrated into the intima, modified LDL is consumed by macrophages causing a decrease in the concentration of modified LDL. We notice that in Fig. 3a, the larger the value of  $\sigma_m$  is, the earlier the concentration of modified LDL begins to decrease and the lower the concentration of modified LDL throughout the intima at the steady state.

There are two key features in the chemoattractant concentration at the endothelial boundary (Fig. 3b) as  $\sigma_m$  increases. Firstly, over a short time, as we increase  $\sigma_m$ , we get an increase in the chemoattractant concentration. This is most noticeable for the first three  $\sigma_m$  values (blue dashed curve, green solid curve and red dot-dash curve). This is due to the fact that we are getting increasing contributions to the concentration of chemoattractants from macrophage secretion and ES cytokine stimulation of the endothelium. Secondly, once  $\sigma_m$  is above a certain critical value, the steady state chemoattractant concentration at the endothelium begins to decrease as  $\sigma_m$  increases. This is because once modified LDL has been consumed and drops to lower concentrations for the larger values of  $\sigma_m$ , the contribution to chemoattractant concentration via the  $\sigma_{p_1} \frac{\ell}{\beta_p + \ell}$  term is less significant than the production of chemoattractant from macrophage secretion and ES cytokine stimulation of the endothelium. However, the production of chemoattractant from macrophage secretion and ES cytokine stimulation of the endothelium is unable to keep chemoattractant concentrations from decreasing.

The level of chemoattractants controls the monocyte migration into the intima. Figure 3c shows that as  $\sigma_m$  increases, the monocyte migration increases. We note a very interesting feature of Fig. 3c. When comparing the red dot-dash ( $\sigma_m = 7.0 \times 10^{-5}$ ) and magenta dashed ( $\sigma_m = 8.0 \times 10^{-5}$ ) curves, the values for monocyte migration are very similar after the initial phase. Initially, the red dot-dash curve is noticeably beneath that of the magenta dashed curve due to the respective chemoattractant concentrations at early time, where the magenta curve grows more quickly than that of the red curve. However, on the magenta curve, once the chemoattractant decreases to a steady state, the monocyte migration decreases to a steady state also. Thus we conclude that monocyte migration for a low value of  $\sigma_\ell$  switches behaviour from chemoattractant controlled migration to  $\sigma_m$  controlled migration, the availability of monocytes in the lumen that can adhere to the endothelium.

Figure 3d–f illustrate the features of this model that constitute lesion development. In Fig. 3e, increasing  $\sigma_m$  leads to higher consumption rates throughout the intima. For low values of  $\sigma_m$ , there is excess modified LDL in the intima (Fig. 3a), and so this consumption rate is controlled by the number of macrophages within the intima (Fig. 3d), which in turn is controlled by  $\sigma_m$ . Furthermore, Fig. 3e shows, for these larger values of  $\sigma_m$ , that the consumption rate of LDL at the quasi-steady state saturates to a value determined by the influx of LDL into the intima, so that the consumption rate of modified LDL throughout the intima becomes constant. Therefore, values of  $\sigma_m$  that achieve the same limiting consumption rate, have very similar foam cell densities (Fig. 3f).

While modified LDL influx remains low, the transitory inflammatory period is kept relatively short when compared to the larger value of  $\sigma_\ell$  (Fig. 4). For low  $\sigma_\ell$ , (that is, low modified LDL influx) qualitative behaviour changes smoothly as  $\sigma_m$  increases.

This is not the case for higher values of  $\sigma_\ell$ . Figure 4 shows the same set of plots as Fig. 3 but for a higher value of  $\sigma_\ell$ . In Fig. 4,  $\sigma_\ell = 7 \times 10^2$  and  $\sigma_m$  lies in same range as for Fig. 3.

As in Fig. 3, the concentration of modified LDL (Fig. 4a) after initially increasing, decreases to steady state. However, increasing  $\sigma_m$  shows that there is a transition from modified LDL being present in the intima at steady state to essentially no modified LDL in the intima. With all of the curves in Fig. 4 there is a distinct change in the qualitative nature of the solutions over time. This transition occurs between  $\sigma_m = 6.0 \times 10^{-5}$  and  $\sigma_m = 7.0 \times 10^{-5}$ .

Chemoattractant concentration drives this transition (Fig. 4b). For the lower values of  $\sigma_m$  (blue dashed curve and green solid curve), the dynamics are very similar to that of low  $\sigma_\ell$  case (Fig. 3). Modified LDL stimulates the endothelial cells to produce chemoattractants and  $\sigma_m$  is too small to recruit enough monocytes to consume the modified LDL, and so modified LDL dominates the intima.

However, this changes when  $\sigma_m$  increases. The plot of the evolution of the chemoattractant concentration at the endothelial boundary against time has two changes in concavity (Fig. 4b). This suggests that initially the same processes operate for all values of  $\sigma_m$  but for the higher values, an extra process kicks in at about  $\tau = 1.5$  for  $\sigma_m = 7.0 \times 10^{-5}$  and at  $\tau = 0.5$  for  $\sigma_m = 8.0 \times 10^{-5}$ .

Unlike the low  $\sigma_\ell$  case (Fig. 3), the consumption of modified LDL by macrophages contributes significantly to the inflammatory period. The concentration of ES cytokines now becomes significant and contributes to the production of more monocyte chemoattractant by endothelial cell stimulation as well as enhancing monocyte adhesion to the endothelial wall. The higher value of  $\sigma_\ell$  fuels this process.

This change in behaviour is also evident in the monocyte migration (Fig. 4c). The two low values of  $\sigma_m$  are at comparable levels to the low  $\sigma_\ell$  case (Fig. 3), but for the two higher values of  $\sigma_m$ , monocyte migration switches to a much higher levels at quasi-steady state reflecting not only the additional monocyte chemoattractant in the intima, but the action of the ES cytokines in enhanced endothelial adherence.

These monocytes account for the rapid growth in the rate of consumption of modified LDL (Fig. 4e) and a consequent rapid reduction in the concentration of modified LDL on the endothelial boundary (Fig. 4a).

There are two timescales for transients when  $\sigma_m$  and  $\sigma_\ell$  are both high. One is timescale of order  $\tau \sim 1$  which governs monocyte migration, modified LDL concentration and chemoattractant concentration. The other is of order  $\tau \sim 10$  and governs macrophage numbers in the intima (Fig. 4d). We know from other numerical solutions that the total number of macrophages in the intima goes to a constant value as  $\tau \rightarrow \infty$  (not shown in Fig. 4d). The speed at which the solution approaches this value depends on the balance between monocyte migration Fig. 4c, governed by  $\sigma_m$  and the consumption of modified LDL in the formation of foam cells (Fig. 4f), governed by  $\sigma_\ell$  at long time.

Figure 4f shows that foam cell populations at a given time are quite different for small differences in  $\sigma_m$ . Although the same limiting consumption rate is reached for the two largest values of  $\sigma_m$ , the largest value has produced around 30% more foam cells by  $\tau = 4$  as it has reached its maximum production rate more quickly. This is distinctly different from the low  $\sigma_\ell$  case (Fig. 4f).

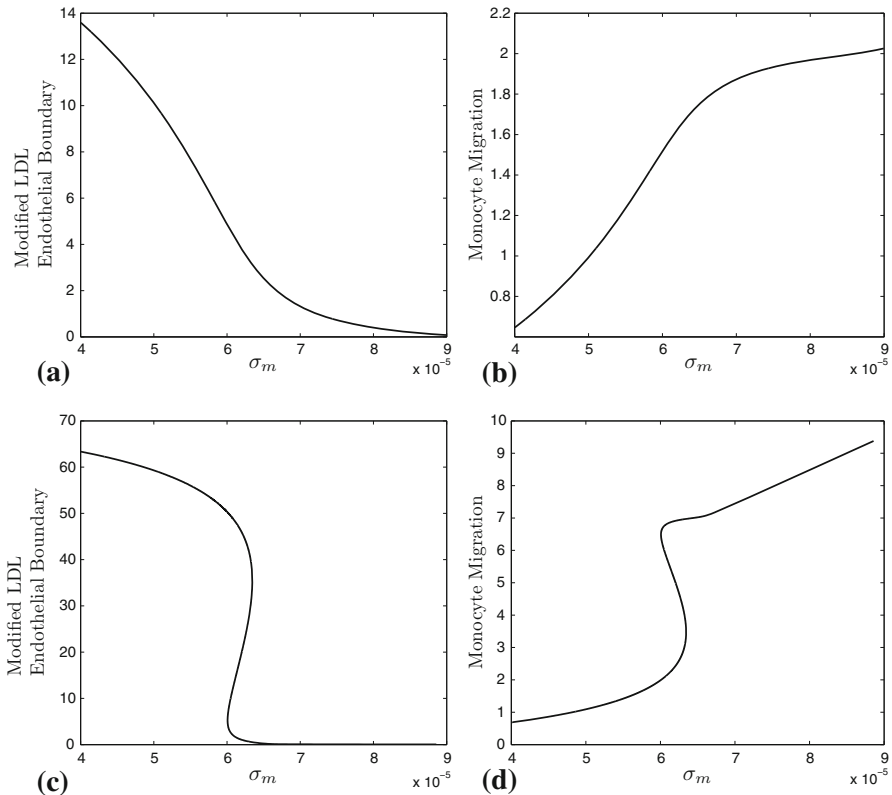


**Fig. 6** Bifurcation plots showing the quasi-steady state values of modified LDL concentration at the endothelial boundary vs  $\sigma_m$  in (a) and (c) and monocyte migration into the intima in (b) and (d). **a** and **b** correspond to Fig. 3, a low  $\sigma_\ell$  value ( $\sigma_\ell = 200$ ); **c** and **d** correspond to Fig. 4, a high  $\sigma_\ell$  value ( $\sigma_\ell = 700$ )

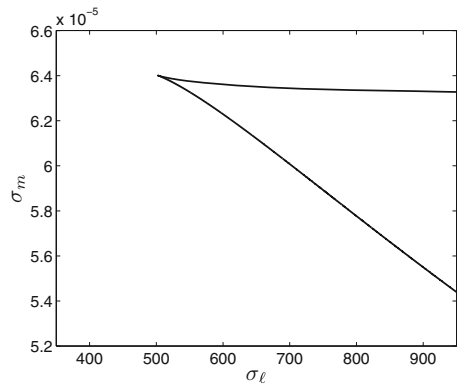
## 6 Bifurcation and bistability in $\sigma_\ell$ - $\sigma_m$ parameter space

In all cases in Figs. 3 and 4 all quantities except foam cell numbers settle to a constant value which we describe as the quasi-steady state. We used AUTO (Doedel et al. 2007) to draw bifurcation diagrams at this quasi-steady state with bifurcation parameter  $\sigma_m$  for  $\sigma_\ell = 2$  and  $7 \times 10^2$ . Figure 6 shows the bifurcation diagrams where the quasi-steady state solutions are measured by modified LDL concentration at the endothelial boundary (cf. Fig. 6a, c) and monocyte migration through the endothelium (cf. Fig. 6b, d).

When  $\sigma_\ell$  is low, the quasi-steady state value of modified LDL at the boundary decreases monotonically with  $\sigma_m$  (Fig. 6a) and monocyte migration increases monotonically (Fig. 6b).

When  $\sigma_\ell$  is large, however, the bifurcation curve has two fold bifurcations and hence there is a switch from high to low values of modified LDL concentration as  $\sigma_m$  increases (Fig. 6c) and from low to high rates of monocyte migration (Fig. 6d). As discussed in Sect. 5, production of chemoattractant is dominated by modified LDL stimulation on the branch with lower  $\sigma_m$  and production through LDL consumption

**Fig. 7** Parameter plot of the loci of fold bifurcations at quasi-steady state as  $\sigma_\ell$  and  $\sigma_m$  change. These curves divide the  $\sigma_\ell - \sigma_m$  parameter space into a region with three steady states and a region with one steady state. The nature of the single steady state changes depending on the value of  $\sigma_m$



and ES cytokine stimulation dominates on the branch when  $\sigma_m$  is high, that is, the upper branch in Fig. 6d.

Numerical simulations suggest that the upper and lower branches of the fold correspond to attracting quasi-steady state solutions and the middle branch is a repeller.

Using AUTO, we plot the locus of the fold points as a function of  $\sigma_\ell$  and  $\sigma_m$  (Fig. 7). There is a cusp point at  $\sigma_\ell \approx 502$  and  $\sigma_m \approx 6.40 \times 10^{-5}$ , thus defining a region where there are three quasi-steady state solutions, two of which are attractors. In the rest of parameter space, there is only one solution which is an attractor. On one side of the region of three steady states, the single quasi-steady state has a high modified LDL concentration and a low macrophage density; on the other side, the single quasi-steady state has a high macrophage density and low modified LDL concentration.

Figure 7 suggests that the bifurcation curves where  $\sigma_\ell$  is taken as the bifurcation parameter for constant  $\sigma_m$  has one or two fold bifurcations. Figure 8 shows the three qualitatively different bifurcation curves for different values of  $\sigma_m$ . For low values of  $\sigma_m$  (Fig. 8c), the attracting quasi-steady state with low monocyte migration and residual modified LDL always exists for all values of  $\sigma_\ell$ . However the repelling quasi-steady state is relatively close to this low steady state which suggests that a comparatively small perturbation of the low steady state will switch the system to the other attracting quasi-steady state with high monocyte migration.

For intermediate values of  $\sigma_m$  (Fig. 8b) there are two folds and the low-inflammation state does not exist for high  $\sigma_\ell$ . This suggests that there is a discontinuous switch in plaque inflammation and growth rates at quasi-steady state as  $\sigma_\ell$  increases or decreases.

When  $\sigma_m$  is high (Fig. 8a) there is only one quasi-steady state. There are no discontinuous switches due to fold bifurcations but inflammation levels increase rapidly as  $\sigma_\ell$  increases.

## 7 Discussion

### 7.1 Plaque growth: interpreting the results of the model

This model is for the earliest events in the formation of atherosclerotic plaque. It does not include the formation of the necrotic core or the collagen cap, but only includes

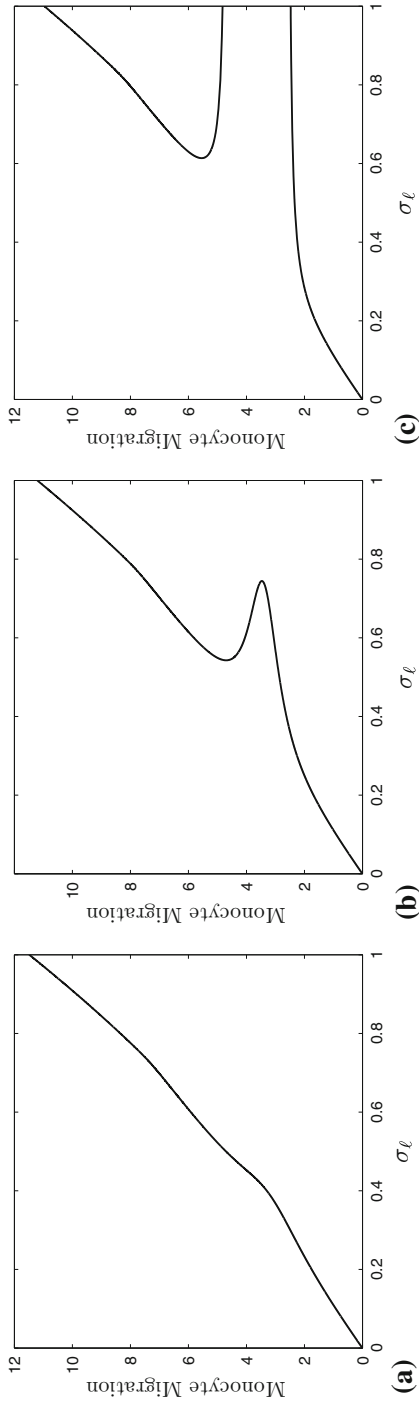


**Fig. 8** Bifurcation plots at quasi-steady state of the total number of macrophages density across the intima, using  $\sigma_\ell$  as a bifurcation parameter. **a** For high  $\sigma_m$  where there are no fold bifurcations; **b** for intermediate value of  $\sigma_m$  where there is a fold and **c** for a low value of  $\sigma_m$  where there is one saddle-node bifurcation

events and species that are active immediately following endothelial injury. The purpose of the model is to explore the events which follow injury and may determine whether the endothelial injury resolves in time or evolves into a large and dangerous plaque over many years.

The first observable sign of atherosclerotic plaque formation is a fatty streak in the wall of the artery (Kharbanda and MacAllister 2005). In this model, the growth in the number of foam cells corresponds to the accumulation of lipids in a fatty streak. Eventually, in real arteries, the fatty streak becomes sufficiently large that foam cells undergo necrosis to form a necrotic core and smooth muscle cells start to move from the media to the endothelial boundary of the intima and produce collagen to form a hard cap (Libby 2002). Once this happens, our model ceases to be valid; a different model is required to capture the fundamental processes in later-stage plaque.

## 7.2 The model agrees qualitatively with known observations

The model correctly predicts that the rate of accumulation of foam cells in most cases, is proportional to the influx of modified LDL into the intima once the initial response to injury has settled down. It also predicts that if there are comparatively high levels of monocytes in the blood stream, then inflammation will persist in the lesion. This agrees with the known correlation between inflammatory diseases, such as uncontrolled diabetes, obesity and osteoarthritis and an increased risk of heart disease (Galkina and Ley 2009; Berg and Scherer 2005; Prior et al. 2014). Inflammation in other parts of the body produces more circulating monocytes in the blood stream.

## 7.3 The role of LDL influx into the intima

The solutions to these equations is driven by the flux of modified LDL into the intima; that is, by the value of  $\sigma_\ell$ . If  $\sigma_\ell = 0$  then all the dependent variables remain zero for all time. This reflects the nature of the problem: if there is no injury to the endothelium and no modification to the entry of LDL particles into the intima, then there is no endothelial or immune cell (monocyte/macrophage) response and no plaque forms.

The parameter  $\sigma_\ell$  which represents the flux of modified LDL into the intima, can be thought of as analogous to the blood LDL cholesterol level that is routinely measured in most older people in developed countries. A high value of  $\sigma_\ell$  corresponds to high LDL cholesterol levels and low  $\sigma_\ell$  corresponds to low LDL cholesterol.

When  $\sigma_\ell$  is low, Fig. 6a and b shows that there is no switch between the uninfamed, high modified LDL/low monocyte migration quasi-steady state and the inflamed, low modified LDL/high monocyte migration steady state and the values of the dependent variables at quasi-steady state change smoothly with changing  $\sigma_m$ , rather than changing discontinuously as in Fig. 6c and d. Hence the model predicts that a low flux of modified LDL into a developing early plaque eliminates the possibility of a switch to a highly inflamed state where the fatty streak grows more rapidly.

Figure 7 suggests that at a high blood monocyte count, the system will necessarily converge to a quasi-steady state where monocyte migration into the plaque is high and so the plaque will grow rapidly unless  $\sigma_\ell$  is very low. For intermediate values of

$\sigma_m$ , Fig. 7 shows that there is an interval of  $\sigma_\ell$  values where there are two attracting and one repelling quasi-steady state solutions for the system so that plaques may be either uninfamed and slow-growing or inflamed and rapidly growing depending on their history. When  $\sigma_m$  is low, the lower branch of solutions always exists, so provided there are no large perturbations to the system, the plaque will always remain in the low inflammation quasi-steady state as  $\sigma_\ell$  changes (Fig. 8c).

These results suggest, not only the importance of keeping LDL cholesterol levels low, but also the importance of maintaining low blood monocyte counts. Even with a constant LDL cholesterol level, a sufficiently sustained change in monocyte count may switch the plaque into a new, highly inflamed state.

#### 7.4 Inflammation: the physiological meaning of monocytes and macrophages

Monocytes are cells of the innate immune system that circulate in the blood stream. They can migrate into other tissues where they differentiate into macrophages. Macrophages have several different subtypes (Tabas 2010), but their most common function is to consume (phagocytose) cellular debris, pathogens and foreign substances. The presence of macrophages is frequently regarded as a marker of inflammation. Macrophages also produce cytokines, including chemoattractants and enzymes such as matrix metalloproteinases (Libby 2002). Matrix metalloproteinases are implicated in plaque rupture in the mature plaque (Newby 2008).

In this paper we refer to this class of immune cells as “monocytes” when they are in the blood stream and as they pass through the endothelium and as “macrophages” once they have entered the intima. It is important, however, to remember that both monocytes and macrophages are essentially the same set of cells, just in different places and at different stages of their development.

We interpret the parameter  $\sigma_m$  to represent not only the availability of monocytes in the bloodstream, but their ability to adhere to an injured endothelium. The flux of monocytes into the intima depends, not only on  $\sigma_m$ , but also on the concentrations of chemoattractant  $p$  and endothelial stimulating (ES) cytokine  $q$  [Eq. (10)], and indirectly on the concentration of modified LDL either through the production of chemoattractant or ES cytokines [Eqs. (5)–(7)]. If there are few circulating monocytes, however, even high levels of chemoattractant and a highly stimulated endothelium will not produce a strong flux of macrophages into the intima.

The number of monocytes in the blood stream is easily quantified by standard tests. Infection in the body can temporarily increase the number of circulating monocytes and chronic diseases such as osteoarthritis and untreated diabetes can produce permanently elevated monocyte counts. It is known that increased monocyte counts are a risk factor in the progression of atherosclerotic plaques (Nozawa et al. 2010).

Our results suggest that there is a switch between a slow-growing uninfamed lesion with a low density of macrophages and a highly inflamed early plaque that grows comparatively quickly. For large values of  $\sigma_m$ —that is, for a high monocyte count—the only solution is for this inflamed, fast-growing plaque. For intermediate values of  $\sigma_m$  both solutions are possible. If a high enough monocyte count is sustained for sufficiently long, then the plaque may switch from the comparatively benign, uninfamed

state to the inflamed, fast growing quasi-steady state and will not return once the monocyte count returns to its former level.

Plaque behaviour similar to this switch is observed clinically in patients who have recently had heart attacks which are known to raise their blood monocyte counts during the months following the heart attack. These patients are at increased risk of further heart attacks during this time (Milonas et al. 2010). A recent study showed that mice who had received a cardiac injury similar to a heart attack subsequently developed larger atherosclerotic lesions and at the same time experienced a sustained increase in the production of monocytes (Dutta et al. 2012). Although this result is for late stage plaque, it does suggest that monocyte availability is crucial in determining plaque progression.

### 7.5 The role of monocyte chemoattractants and endothelial stimulating cytokines

Monocytes chemoattractants, such as MCP-1, are crucial in the development of atherosclerosis. If these are absent, then plaque growth is substantially reduced (Charo and Taubman 2004). We have shown that in this model, highly inflamed plaques have high levels of chemoattractant production and high chemoattractant concentrations.

The presence of adhesion molecules such as VCAMs and ICAMs on cells of the damaged endothelium is also vital for the recruitment of monocytes (Galkina and Ley 2007). Endothelial stimulating cytokines increase the density of adhesion molecules on the endothelium and increase the production of chemoattractant by the endothelium but their presence is not essential for the entry of monocytes into the intima. For this reason we have focused primarily on the chemoattractant rather than the ES cytokines.

Nevertheless the ES cytokines have a noticeable effect on the dynamics. For example they substantially increase monocyte immigration into the intima, especially in the highly inflamed state where large amounts of ES cytokine is being produced in the intima as macrophages consume modified LDL.

### 7.6 The choice of bifurcation parameters

In Sect. 5, we looked at how model outputs varied as the influx of modified LDL into the intima,  $\sigma_\ell$ , and the availability of monocytes  $\sigma_m$  were changed. These are quantities that correlate with clinically measurable factors such as LDL cholesterol in the blood and blood monocyte count. From a mathematical point of view, we could equally well have looked at the role of any other parameters. Possibly the most interesting of these are the parameters that govern the rate of consumption of modified LDL by macrophages,  $\mu_\ell$  and the rate that macrophages turn into foam cells due to modified LDL consumption,  $\mu_m$ . These affect the way that modified LDL, macrophage numbers and other quantities evolve in the transient phase but the bifurcation diagrams for solutions at the quasi-steady are similar. This is because the levels of modified LDL and macrophages at quasi-steady state are determined by the balance between modified LDL present in the intima and the availability of macrophage capacity to consume modified LDL. This balance can either be determined by the influx into the intima of modified LDL and monocytes (that become macrophages) or by the rate at which modified LDL is

consumed once it is in the intima balanced with the dwelling time of macrophages in the intima which is primarily determined by the rate at which they become foam cells.

### 7.7 Other factors that affect inflammation and plaque progression

As the model stands, when there are two possible stable quasi-steady states, then one has high modified LDL concentrations and low macrophage density and the other has high macrophage density and low modified LDL concentration (see Fig. 6). This suggests that there is a discontinuous switch in macrophage recruitment as monocyte availability increases. Either there are enough macrophages in the intima to consume modified LDL at a sufficient rate to produce enough chemoattractant to recruit more macrophages and so support a high macrophage population that can consume all the modified LDL present or macrophage levels are too low to consume all the modified LDL and also to produce sufficient chemoattractant to foster more recruitment. In this case, chemoattractant is primarily produced by the modified LDL that remains unconsumed at the endothelium. Unless more macrophages can be recruited, then modified LDL concentration will stay high and macrophages density low.

In actual lesions there are factors that enable extra activity at low macrophage density to prevent high modified LDL concentrations in the intima and there are anti-inflammatory factors that limit the density of macrophages when they dominate the intima.

The presence of modified LDL in a lesion continues to excite the endothelium which continues to express adhesion molecules. These attach, not only to monocytes but also to *T* cells, which also penetrate the endothelium to the intima. These *T* cells respond to the presence of modified LDL by producing pro-inflammatory cytokines that stimulate the endothelium to produce more adhesion molecules and increase the activity of the macrophages (Hansson and Libby 2006). For simplicity this model does not include *T* cells, but if they were included in a more complicated model, we expect that the solution with modified LDL remaining present in the intima would exist only in a smaller region of parameter space. This *T* cell feedback is included in an earlier ODE model (Ougrinovskaia et al. 2010).

In real lesions there exist classes of *T* cells and macrophages that produce anti-inflammatory cytokines, transforming growth factor  $\beta$  (TGF- $\beta$ ) and interleukin-10 (IL-10). TGF- $\beta$  limits the recruitment of monocytes to the lesion and both TGF- $\beta$  and IL-10 reduce the activity of macrophages (Andersson et al. 2010). This, along with other healing processes can enable a fatty streak to regress and inhibit the formation of a mature plaque. This model does not include this anti-inflammatory phase, but clearly, if it would be possible to add another class of cytokines to a more comprehensive model.

This model also does not include the action of high density lipoproteins (HDL). HDL has a number of important anti-inflammatory effects: it reduces the excitation of the endothelium; it reduces the rate of modification of LDL; it exports lipids from foam cells (and, indeed it provides really the only mechanism for this) and it enables foam cells and macrophages to leave the intima (Llodra et al. 2004). ODE modelling (Cohen et al. 2014) suggests that lipid export and cell emigration, particular can have a significant impact of plaque inflammation and growth or regression.

## 7.8 Moving from a qualitative to quantitative modelling

Although we have attempted to find and use parameter values that lie, at least, within an order of magnitude of their probable value, this model is principally a qualitative model rather than a model that makes correct quantitative predictions. For this model to become quantitatively useful, observations need to be made to find out reaction rates, consumption rates, influx rates and so on *in vivo*. Many of these measurements would be difficult, if not impossible to do dynamically and it is likely that most information would need to be inferred from *post mortem* measurement. Parameter values are easiest to find for mice, rather than humans for ethical reasons. It is impossible to reproduce many aspects of atherosclerosis *in vitro* where measurement is comparatively easy. If, however, some parameters can be accurately determined, it would be possible to find others by fitting model results to observations.

## 7.9 Comparison with other models and analyses

This model includes complicated interactions between the cells in the damaged endothelium but does not include the effect of blood flow. It represents a middle way between simple models that are amenable to analysis, such as the suites of models by [EI Khatib et al. \(2009, 2012\)](#), [Calvez et al. \(2009\)](#) and [Hidalgo et al. \(2014\)](#) and more complicated models that link blood flow with events in the intima by explicitly modelling blood flow and LDL transport in the bloodstream and into the intima such as the collection of models by [Filipovic et al. \(2012, 2013\)](#), [Parodi et al. \(2012\)](#) and [Bulelzai and Dubbeldam \(2012\)](#). These latter models use simple modelling for the inflammatory response.

The aim of the model that we present here is to explore the dynamics of inflammation in early atherosclerosis in more realistic detail than [EI Khatib et al. \(2009, 2012\)](#) or [Calvez et al. \(2009\)](#). We do not include blood flow, but start with the assumption that the endothelium is already injured and letting LDL into the blood vessel wall. We explicitly include the rate of penetration of modified LDL, which allows us to explore the effect of changes in blood LDL on lesion growth and we assume that monocyte availability can be modelled, reflecting the level of inflammation in the body, another clinical concern in the treatment and prevention of atherosclerosis.

In the models [EI Khatib et al. \(2009, 2012\)](#) and [Calvez et al. \(2009\)](#), it is assumed that the recruitment of monocytes from the bloodstream into the intima is saturating while the production of chemoattractant and the consumption of modified LDL by macrophages is bilinear. We assume that the consumption of modified LDL by macrophages and the consequent production of chemoattractant and ES cytokines is saturating in the concentration of modified LDL so each cell has a maximum rate of modified LDL consumption, regardless of the concentration of modified LDL available. We also assume that the entry of monocytes into the intima, is controlled by the concentrations of chemoattractant and ES cytokines in a bilinear way and that the availability of monocytes in the blood stream is controlled directly by a parameter  $\sigma_m$  rather than implicitly assuming a saturating rate of monocyte entry.

[EI Khatib et al. \(2009, 2012\)](#) analyse their model using a travelling wave coordinates and show that there are regions of parameter space where bistability exists and

other regions where there is only one stable positive steady state. [Hidalgo et al. \(2014\)](#) confirms this result with extensive numerical work and confirms that, where bistability exists, the initial conditions determine whether the system settles to the higher or lower steady state. [El Khatib et al. \(2012\)](#) show that this bistability arises via a pitchfork bifurcation. With our more sophisticated model we have shown that hysteresis folds are possible when  $\sigma_m$  is changed for some values of  $\sigma_\ell$  (Fig. 6) and that for increasing values of  $\sigma_m$  the bifurcation diagrams with  $\sigma_\ell$  as the bifurcation parameter give the degenerate unfolding of a pitchfork (Fig. 8). This suggests, not only that initial conditions are important but that subsequent slow changes in parameters may, at critical values, promote rapid changes in lesion inflammation or growth rate.

## 8 Conclusion: The role of nonlinear dynamics in atherosclerosis

This model strongly suggests that dynamics matter in the progression, treatment and outcome of atherosclerosis. We know that plaque growth and inflammation is the outcome of many complicated biochemical and cellular processes both at the endothelium and in the intima and also in other parts of the body via cells and cytokines carried by the blood stream ([Libby 2002](#)). It is therefore no surprise that even a comparatively simple model such as this can produce dramatic changes in behaviour for small changes in parameters. These changes are both in the quasi-steady state levels of modified LDL and macrophage numbers in the intima and in the time that system takes to evolve to quasi-steady state via an initial transient, following injury to the endothelium. Previous ODE models ([Ougrinovskaia et al. 2010](#); [Cohen et al. 2014](#)) have produced similar highly nonlinear effects, in response to changing uptake dynamics ([Ougrinovskaia et al. 2010](#)) and changing high density lipoprotein (HDL) levels ([Cohen et al. 2014](#)). Together, these suggest that it may be unreasonable to expect a linear response to therapies, such as raising HDL or lowering LDL or inflammation. A small change in therapy may produce a major reaction or it may produce no change at all, depending on the underlying dynamics in a particular patient. This suggests that in the long term there may be a role for patient specific therapy for atherosclerosis.

We present here a model that explicitly examines inflammatory events in the intima and interactions between the injured endothelium and the dynamics of cells and cytokines in the intima in response to modified LDL penetration. The long term purpose of this modelling is to provide insight into the effects of treatment regimes and preventative advice and to provide a complementary tool to support research using animal models and clinical studies.

## References

- Andersson J, Libby P, Hansson G (2010) Adaptive immunity and atherosclerosis. *Clin Immunol* 134(1, SI):33–46
- Berg A, Scherer P (2005) Adipose tissue, inflammation, and cardiovascular disease. *Circ Res* 96(9):939–949
- Bulelzai M, Dubbeldam J (2012) Long time evolution of atherosclerotic plaques. *J Theor Biol* 297:1–10
- Bulelzai M, Dubbeldam J, Meijer H (2014) Bifurcation analysis of a model for atherosclerotic plaque evolution. *Phys D-Nonlinear Phenom* 278:31–43

- Calvez V, Ebde A, Meunier N, Raoult A (2009) Mathematical modelling of the atherosclerotic plaque formation. *ESAIM Proc* 28:1–12
- Calvez V, Houot J, Meunier N, Raoult A, Rusnakova G (2010) Mathematical and numerical modeling of early atherosclerotic lesions. *ESAIM Proc* 30:1–14
- Channon K (2002) The endothelium and the pathogenesis of atherosclerosis. *Medicine* 30(4):54–58
- Charo I, Taubman M (2004) Chemokines in the pathogenesis of vascular disease. *Circ Res* 95(9):858–866
- Cilla M, Pena E, Martinez M (2014) Mathematical modelling of atheroma plaque formation and development in coronary arteries. *J R Soc Int* 11(90):20130866
- Cobbold C, Sherratt J, Maxwell S (2002) Lipoprotein oxidation and its significance for atherosclerosis: a mathematical approach. *Bull Math Biol* 64(1):65–95
- Cohen A, Myerscough M, Thompson R (2014) Athero-protective effects of high density lipoproteins (HDL): an ODE model of the early stages of atherosclerosis. *Bull Math Biol* 76(5):1117–1142
- Dabagh M, Jalali P, Tarbell J (2009) The transport of LDL across the deformable arterial wall: the effect of endothelial cell turnover and intimal deformation under hypertension. *Am J Physiol-Heart Circ Physiol* 297(3):H983–H996
- Di Vito L, Porto I, Burzotta F, Trani C, Pirozzolo G, Niccoli G, Leone AM, Crea F (2013) Radial artery intima-media ratio predicts presence of coronary thin-cap fibroatheroma: A frequency domain-optical coherence tomography study. *Int J Cardiol* 168(3):1917–1922
- Doedel E, Champneys A, Fairgrieve T, Kuznetsov Y, Oldeman B, Paffenroth R, Sandstede B, Wang X, Zhang C (2007) AUTO-07P: continuation and bifurcation software for ordinary differential equations. <http://cmvl.cs.concordia.ca/>. Accessed Oct 2012
- Dutta P, Courties G, Wei Y, Leuschner F, Gorbатов R, Robbins C, Iwamoto Y, Thompson B, Carlson A, Heidt T, Majmudar M, Lasitschka F, Etzrodt M, Waterman P, Waring M, Chicoine A, van der Laan A, Niessen H, Piek J, Rubin B, Butany J, Stone J, Katus H, Murphy S, Morrow D, Sabatine M, Vinegoni C, Moskowitz M, Pittet M, Libby P, Lin C, Swirski F, Weissleder R, Nahrendorf M (2012) Myocardial infarction accelerates atherosclerosis. *Nature* 487(7407):325–329
- El Khatib N, Genieys S, Volpert V (2007) Atherosclerosis initiation modeled as an inflammatory process. *Math Model Nat Phenom* 2(2):126–141
- El Khatib N, Genieys S, Kazmierczak B, Volpert V (2009) Mathematical modelling of atherosclerosis as an inflammatory disease. *Philos Trans R Soc A-Math Phys Eng Sci* 367(1908):4877–4886
- El Khatib N, Genieys S, Kazmierczak B, Volpert V (2012) Reaction–diffusion model of atherosclerosis development. *J Math Biol* 65(2):349–374
- Filipovic N, Rosic M, Tanaskovic I, Milosevic Z, Nikolic D, Zdravkovic N, Peulic A, Kojic M, Fotiadis D, Parodi O (2012) ARTreat project: three-dimensional numerical simulation of plaque formation and development in the arteries. *IEEE Trans Inf Technol Biomed* 16(2, SI):272–278
- Filipovic N, Nikolic D, Saveljic I, Milosevic Z, Exarchos T, Pelosi G, Parodi O (2013) Computer simulation of three-dimensional plaque formation and progression in the coronary artery. *Comput Fluids* 88:826–833
- Fok P (2012) Mathematical model of intimal thickening in atherosclerosis: vessel stenosis as a free boundary problem. *J Theor Biol* 314:23–33
- Furchgott R (1999) Endothelium-derived relaxing factor: discovery, early studies, and identification as nitric oxide. *Biosci Rep* 19(4):235–251
- Galkina E, Ley K (2007) Vascular adhesion molecules in atherosclerosis. *Arterioscler Thromb Vasc Biol* 27(11):2292–2301
- Galkina E, Ley K (2009) Immune and inflammatory mechanisms of atherosclerosis. *Ann Rev Immunol* 27:165–197
- Gessaghi V, Raschi M, Tanoni D, Perazzo C, Larreteguy A (2011) Growth model for cholesterol accumulation in the wall of a simplified 3D geometry of the carotid bifurcation. *Comput Methods Appl Mech Eng* 200(23–24):2117–2125
- Han K, Hong K, Park J, Ko J, Kang D, Choi K, Hong M, Park S, Park S (2004) C-reactive protein promotes monocyte chemoattractant protein-1-mediated chemotaxis through upregulating CC chemokine receptor 2 expression in human monocytes. *Circulation* 109(21):2566–2571
- Hansson G, Libby P (2006) The immune response in atherosclerosis: a double-edged sword. *Nat Rev Immunol* 6(7):508–519
- Hidalgo A, Tello L, Toro E (2014) Numerical and analytical study of an atherosclerosis inflammatory disease model. *J Math Biol* 68(7):1785–1814

- Ibragimov A, McNeal C, Ritter L, Walton J (2005) A mathematical model of atherogenesis as an inflammatory response. *Math Med Biol-A J IMA* 22(4):305–333
- Kharbanda R, MacAllister R (2005) The atherosclerosis time-line and the role of the endothelium. *Curr Med Chem Immunol Endocr Metab Agents* 5(1):47–52
- Libby P (2002) Inflammation in atherosclerosis. *Nature* 420(6917):868–874
- Libby P, Ridker P (2006) Inflammation and atherothrombosis—from population biology and bench research to clinical practice. *J Am Coll Cardiol* 48(9, Suppl. A):A33–A46
- Little M, Gola A, Tzoulaki I (2009) A model of cardiovascular disease giving a plausible mechanism for the effect of fractionated low-dose ionizing radiation exposure. *PLOS Comput Biol* 5(10):e1000539
- Llodra J, Angeli V, Liu J, Trogan E, Fisher E, Randolph G (2004) Emigration of monocyte-derived cells from atherosclerotic lesions characterizes regressive, but not progressive, plaques. *Proc Natl Acad Sci USA* 101(32):11,779–11,784
- Lusis A (2000) Atherosclerosis. *Nature* 407(6801):233–241
- McKay C, McKee S, Mottram N, Mulholland T, Wilson S, Kennedy S, Wadsworth R (2004) Towards a model of atherosclerosis. In: Tech. rep. University of Strathclyde
- McKellar G, McCarey D, Sattar N, McInnes I (2009) Role for TNF in atherosclerosis? Lessons from autoimmune disease. *Nat Rev Cardiol* 6(6):410–417
- Milonas C, Jernberg T, Lindback J, Agewall S, Wallentin L, Stenestrand U (2010) Effect of angiotensin-converting enzyme inhibition on 1 year mortality and frequency of repeat acute myocardial infarction in patients with acute myocardial infarction. *Am J Cardiol* 105(9):1229–1234
- Napoli C, de Nigris F, Williams-Ignarro S, Pignalosa O, Sica V, Ignarro L (2006) Nitric oxide and atherosclerosis: an update. *Nitric Oxide-Biol Chem* 15(4):265–279
- Newby A (2008) Metalloproteinase expression in monocytes and macrophages and its relationship to atherosclerotic plaque instability. *Arterioscler Thromb Vasc Biol* 28(12):2108–2114
- Newby A, Zaltsman A (1999) Fibrous cap formation or destruction—the critical importance of vascular smooth muscle cell proliferation, migration and matrix formation. *Cardiovasc Res* 41(2):345–360
- Nozawa N, Hibi K, Endo M, Sugano T, Ebina T, Kosuge M, Tsukahara K, Okuda J, Umemura S, Kimura K (2010) Association between circulating monocytes and coronary plaque progression in patients with acute myocardial infarction. *Circ J* 74(7):1384–1391
- Ougrinovskaia A, Thompson R, Myerscough M (2010) An Ode model of early stages of atherosclerosis: mechanisms of the inflammatory response. *Bull Math Biol* 72(6):1534–1561
- Paavola C, Hemmerich S, Grunberger D, Polsky I, Bloom A, Freedman R, Mulkins M, Bhakta S, McCarley D, Wiesent L, Wong B, Jarnagin K, Handel T (1998) Monomeric monocyte chemoattractant protein-1 (MCP-1) binds and activates the MCP-1 receptor CCR2B. *J Biol Chem* 273(50):33,157–33,165
- Pai J, Pischon T, Ma J, Manson J, Hankinson S, Joshipura K, Curhan G, Rifai N, Cannuscio C, Stampfer M, Rimm E (2004) Inflammatory markers and the risk of coronary heart disease in men and women. *N Engl J Med* 351(25):2599–2610
- Pappalardo F, Musumeci S, Motta S (2008) Modeling immune system control of atherogenesis. *Bioinformatics* 24(15):1715–1721
- Parodi O, Exarchos T, Marraccini P, Vozzi F, Milosevic Z, Nikolic D, Sakellarios A, Siogkas P, Fotiadis D, Filipovic N (2012) Patient-specific prediction of coronary plaque growth from CTA angiography: a multiscale model for plaque formation and progression. *IEEE Trans Inf Technol Biomed* 16(5, SI):952–965
- Plank M, Wall D, David T (2007) The role of endothelial calcium and nitric oxide in the localisation of atherosclerosis. *Math Biosci* 207(1):26–39
- Poston R, Poston D (2007) Typical atherosclerotic plaque morphology produced in silico by an atherogenesis model based on self-perpetuating propagating macrophage recruitment. *Math Model Nat Phenom* 2(2):142–149
- Prior JA, Jordan KP, Kadam UT (2014) Associations between cardiovascular disease severity, osteoarthritis co-morbidity and physical health: a population-based study. *Rheumatology* 53(10):1794–1802
- Ross R (1999) Mechanisms of disease—atherosclerosis—an inflammatory disease. *N Engl J Med* 340(2):115–126
- Tabas I (2010) Macrophage death and defective inflammation resolution in atherosclerosis. *Nat Rev Immunol* 10(1):36–46
- Volpert V, Petrovskii S (2009) Reaction–diffusion waves in biology. *Phys Life Rev* 6(4):267–310
- Zohdi T, Holzapfel G, Berger S (2004) A phenomenological model for atherosclerotic plaque growth and rupture. *J Theor Biol* 227(3):437–443